



Development of X-ray Tracer Diagnostics for Radiatively-Driven Ablator Experiments

**J.J. MacFarlane, D.H. Cohen, Ping Wang, G.A. Moses,
R.R. Peterson, P.A. Jaanimagi, O.L. Landen, R.E. Olson,
T.J. Murphy, G.R. Magelssen, N.D. Delamater**

June 1999

UWFDM-1100

***FUSION TECHNOLOGY INSTITUTE
UNIVERSITY OF WISCONSIN
MADISON WISCONSIN***

Development of X-ray Tracer Diagnostics for Radiatively-Driven Ablator Experiments

Joseph J. MacFarlane*, Principal Investigator
Fusion Technology Institute, University of Wisconsin-Madison
1500 Engineering Drive, Madison WI 53706

Co-Investigators

David H. Cohen*, Ping Wang[†], Gregory A. Moses, Robert R. Peterson
Fusion Technology Institute, University of Wisconsin-Madison

Collaborators

Paul A. Jaanimagi
Laboratory for Laser Energetics

Otto L. Landen
Lawrence Livermore National Laboratory

Richard E. Olson
Sandia National Laboratory

Thomas J. Murphy, Glenn R. Magelssen, Norman D. Delamater
Los Alamos National Laboratory

June 1999

UWFDM-1100

*current address: Prism Computational Sciences, 16 N. Carroll St., Madison, WI 53703.

[†]current address: Allstate Insurance Co., G6A, 3075 Sanders Rd., Northbrook IL 60062.

Contents

FY 1998 NLUF Statement of Work	1
1. Introduction	2
2. Target Design and Development	5
3. Diagnostics	8
4. Experiments and Data	10
4.1. Shock Breakout Shots	11
4.2. Spectroscopy Shots	11
5. Discussion and Conclusions	14
References	17

FY 1998 NLUF Statement of Work

1. Target fabrication:
 - a) Thin-walled hohlraums from General Atomics (GA);
 - b) Witness plate fabrication at GA;
 - c) Bismuth and thorium backlighter foils from Goodfellow Metals;
 - d) Target assembly at LANL and LLNL.
2. Diagnostic development—build LXS.
3. Three days of shots in August 1998.
4. Data analysis and modeling—hohlraum physics and witness plate physics.
5. Presentation of results—APS DPP meeting in New Orleans, November 1998 (2 posters)

1. Introduction

This report covers fiscal year 1998 of our ongoing project to develop tracer X-ray spectroscopic diagnostics for hohlraum environments. This effort focused on an experimental campaign carried out at OMEGA on 25 – 27 August 1998. This phase of the project heavily emphasized experimental design, diagnostic development, and target fabrication, as well as building up numerical models for the experiments. The spectral diagnostic under development involves using two thin (few 1000 Å) mid-Z tracers in two witness plates mounted on the side of a hohlraum with the tracers' K_α absorption features seen against an X-ray backlighter. The absorption data are used to sample the time-dependent, localized properties of each witness plate as a radiation wave ablates it. The experiments represented the first application of this diagnostic, in this case two side-by-side doped and undoped plastic samples to investigate the effects of capsule ablator dopants.

Backlit absorption spectroscopy is a useful diagnostic technique, widely applied to ICF plasmas [1]. Because this technique does not rely on self-emission, it is possible to measure absorption signals from relatively cold material. Measuring inner-shell features in absorption is an excellent means for determining the ionization balance in a material sample because features arising from the same ionization stage appear at similar wavelengths. With features from adjacent ionization stages shifted a small amount in wavelength, the resulting spectrum viewed at a resolution of several hundred, consists of a series of broad absorption features, one for each ionization stage, with the ionization stages inversely proportional to wavelength. Such K_α absorption spectra have been used as a diagnostic in heat transfer experiments [2], laser heating experiments [3], and ion beam experiments [4]. A simulation of the type of time-dependent spectra we expect to record is shown in Figure 1.

By monitoring K_α absorption from a thin tracer layer on the interior of a sample, one can probe the time-dependent ionization conditions at a specific physical location in some material. When either a spherical capsule or a planar witness plate is exposed to a hohlraum radiation field, a radiation wave is launched into the material. This radiation wave drives a shock ahead of it, so that material at a given depth is first modestly heated by the shock and then much more strongly heated by the radiation front. Both these transitions in temperature (and associated ionization) are very rapid. By monitoring the K_α absorption spectrum of a buried tracer, the time at which the radiation wave arrives at the tracer can be determined. The subsequent evolution of the ionization balance in the tracer provides information about the strength of the local radiation field at later times. K_α features of low-Z tracers or K_β features of mid-Z materials can also be used to diagnose the shock arrival time and strength, and possibly even to detect radiation pre-heat ahead of the shock front.

In the case of an ICF capsule, the interaction of the hohlraum radiation field with the low-Z capsule ablator governs the shock compression of the D-T fuel in the interior of the capsule. The speed at which the shock and the radiation wave propagate and the ablation rate can all be controlled (and optimized for efficient capsule implosion) by doping the ablator material with denser, higher opacity mid-Z elements. The enhanced opacity from dopants can also help to mitigate radiation pre-heat of the fuel capsules. For NIF capsules, candidate designs include beryllium ablators doped with copper and polyimide ablators doped with germanium or bromine [5].

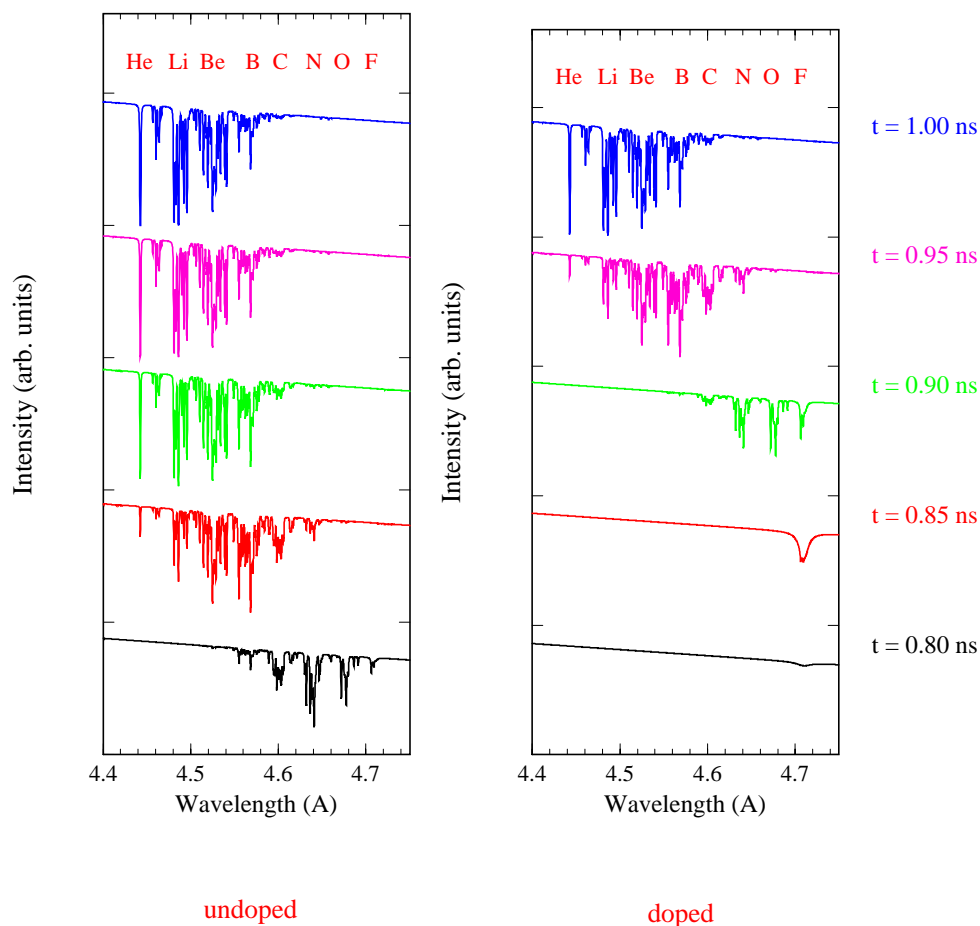


Figure 1. Predicted K_{α} absorption spectra from a chlorine tracer in both a doped and an undoped witness plate. Note the delay in the turn on of the tracer signal in the doped side, through which the radiation wave propagates more slowly. Also note the distinct absorption complexes, one for each ionization stage, evolve relatively quickly in time. Although in the actual experiments, we will have two different tracers, one in each witness plate, we show the same tracer here to emphasize the different behavior of the doped and undoped samples.

Clearly, it is important to understand how the hohlraum X-rays interact with the ablator material, and specifically, what the effects of the dopants are. In order to simplify the geometry, and isolate the effects of the dopants, one can place planar samples of ablator materials (witness plates) on the sides of hohlraums. And instead of using a pulse shape tailored for a capsule implosion, a simple flat-top laser profile can be used. Ideally, one would like to compare multiple samples, with varying dopant levels, exposed to the same hohlraum radiation field. To obtain time-dependent spectra with spatial information (from two different samples on the same hohlraum) would require three dimensions of data (time-wavelength-space), which, it would seem, cannot be simultaneously monitored on a single two dimensional detector (film). However, by placing two different tracer substances, one in each witness plate, it is possible to use spectral information as a proxy for spatial information. In other words, the K_α absorption signals from the two different witness plates will appear in two distinct portions of the spectrum due to the different tracers employed. In this way, a time-resolved 2-dimensional spectrum contains information about the time-evolution of the ionization balance in each of the two tracers (and thus in each of the two witness plates).

Our goal then is to develop the backlit K_α tracer absorption diagnostic for side-by-side samples, and apply it to a comparison of doped and undoped capsule ablator materials. Applications to other kinds of materials in other types of environments (e.g. Z-pinch) will eventually also be possible. We also note that this project is in some ways a continuation of earlier work on the NOVA laser with tracer emission spectroscopy [6]. In order to make a meaningful measurement of the ablator samples, we need to be able to characterize the time-dependent hohlraum conditions. Additionally, it would help to constrain the analysis of the performance of the ablator samples if we had other experimental constraints on their response to the hohlraum radiation field. For that reason, our experimental campaign included a subset of targets with wedge-shaped witness plates (without any tracers), for which we made shock breakout measurements in doped and undoped samples. In these shots we also monitored the hohlraum temperatures using DANTE. By combining the absorption spectroscopy, the shock breakout information, and the hohlraum radiation conditions we hope to be able to constrain the time-dependent conditions in the ablator samples quite well.

Much of the work covered in this report involved the planning and design of these relatively complex experiments, including target design and fabrication. Although the actual experiments were not completely successful, much was accomplished. This diagnostic development program is continuing in fiscal year 1999, with another experimental campaign planned for July 1999. And in March 1999 we shot a small number of targets with tracers buried only 1 to 2 μm from the front of plastic witness plates, and verified that we could measure a K_α absorption signal in our experimental configuration. The remainder of this report will concentrate on the details of the targets, the diagnostic instruments, the measurements, and the modeling.

Table 1. Witness Plate Properties

	Undoped (GDP)	Doped (GDP+Ge)
density (g cm ⁻³)	1.03	1.27
C fraction (atomic)	0.40	0.39
H fraction (atomic)	0.56	0.55
O fraction (atomic)	0.04	0.04
Ge fraction (atomic)	0.00	0.0175

2. Target Design and Development

We chose to work with germanium-doped plastic ablator samples, as plastic target fabrication was more advanced than was copper-doped beryllium fabrication at the time we were designing the targets. We had extensive discussions with various people at the University of Wisconsin (UW), GA, and the national labs, including Pete Gobby and Russ Wallace about target fabrication techniques. The greatest challenge was building the planar plastic witness plates, which effectively consisted of three layers: 20 μm to 40 μm of plastic (doped or undoped), then a sub-micron thick tracer layer consisting of NaCl or KF, and then another layer of plastic 10 μm to 20 μm thick, having the same composition as the first layer.

Ultimately we charged Abbas Nikroo and Jim Kaae of GA with the task of fabricating the targets using glow discharge polymerization (GDP) to make the witness plates. The GDP was used to build the initial, thicker layer of plastic (several cm square). Then this planar sample was coated with the salt layer using vacuum deposition. Next, the salt-coated sample was put back in the GDP machine and an additional layer of plastic was applied. The three-layer samples were then cut into individual witness plates 400 μm by 800 μm . Finally, the outer surfaces of the witness plates were machined smooth, with a r.m.s. thickness variation of less than 1 μm .

There was concern about the ability of the final GDP layer to adhere to the coated sample. There were some problems, especially with the KF-coated plastic. Although the final layer did ultimately adhere, in some samples there were air pockets up to 5 μm thick between the plastic layers, as revealed by electron microscopy. Fortunately enough samples without this problem were produced. The electron microscope also revealed that much of the salt layer had formed into dense, but irregular clumps, probably due to contamination by water. These clumps had spatial scales of several tens of microns, and the backlighter beam width is more than this, so our spectra would effectively average out these irregularities. The thicknesses of the plastic layers of each witness plate were measured using interferometry. The compositions and densities of the doped and undoped witness plates are summarized in Table 1. The tracer layers were estimated to be slightly over 5000 \AA thick. At $\rho \approx 2 \text{ g cm}^{-3}$, this corresponds to K and Cl column densities of $10^{-4} \text{ g cm}^{-2}$ or $2 \times 10^{18} \text{ ions cm}^{-2}$.

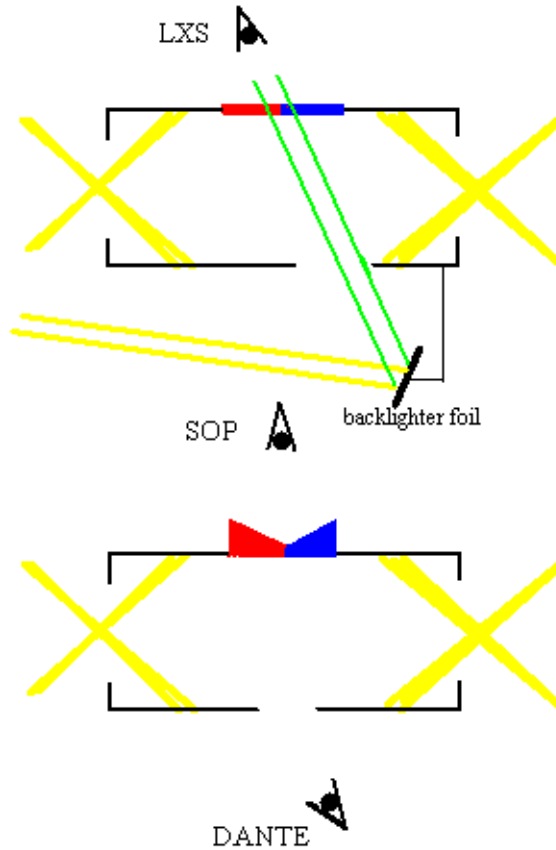


Figure 2. Schematic illustration of the hohlraum, packages, and diagnostics for our two types of proposed targets: spectroscopy (top) and shock-breakout (bottom). Note the backlighter foil attached to the hohlraum on the spectroscopy targets, which converts laser light (yellow) to x-rays (green), that then propagate through the hohlraum, through the two witness plates (red and blue) and on to the spectrometer. These sketches are not drawn to scale.

The shock breakout targets did not have tracer layers, and were thus easier to fabricate. Flat GDP samples roughly $50\ \mu\text{m}$ thick were made in exactly the same way as the first layer of the tracer spectroscopy targets. These were then cut into individual witness plates and micro-machined into wedges with thicknesses varying from somewhat less than $20\ \mu\text{m}$ at one end to roughly $50\ \mu\text{m}$ at the other.

In Figure 2 we show schematic diagrams of the two different types of targets that we shot in the August 1998 campaign. These diagrams demonstrate some of the basic issues we faced in designing the experiments.

The two different witness plates (ablator samples) were placed side-by-side on the “flat” on the side of the hohlraums. Our absorption backlighting scheme involves point-projection spectroscopy [1], of each of the two samples. Because the same spectrometer was observing both backlighter beams, we needed two separate small area backlighters. The single backlighter structure that can be seen in the top sketch in Figure 2 actually contains

two different foils, each illuminated by a set of three OMEGA beams. By focusing the three beams at the same point on each of the foils, we produced a region of hot plasma no more than $100\ \mu\text{m}$ in diameter. The experiment's duration was no more than 2 ns, so expansion of the plasma was not a major problem. The $100\ \mu\text{m}$ spot size was small enough to keep the source broadening component of the spectral resolution small compared to the inherent instrumental resolution. The backlighter spot separation was comparable to the distance between the centers of the two witness plates ($500\ \mu\text{m}$), and the X-ray backlighter beams propagate through the hohlraum (via a hole drilled into the barrel of the hohlraum), through the two witness plates, and into the spectrometer, at roughly the same acceptance angle (the spectrometer design will be discussed in the following section).

The backlighters needed to have strong quasi-continuum emission at the wavelengths of the K_α absorption features of the corresponding tracers. And preferably very little emission at the wavelength of the other tracer, so that the signal from a given tracer would not be contaminated by emission from the other backlighter. Additionally, the tracer K_α features needed to be at wavelengths that are long enough so that an appropriate backlighter can be found, but short enough so that the bound-free opacity of the ablator samples (especially in the doped sample) was not too severe. This spectral window corresponds to roughly $3\ \text{\AA}$ (where the uranium M-shell emission plateau is) to roughly $5\ \text{\AA}$, where the germanium L-shell bound-free edge is.

Chlorine ($Z=17$) is a good candidate for a tracer, as its K_α features are near $4.6\ \text{\AA}$. Additionally, Cl K_α has been seen in absorption against bismuth ($Z=83$) M-shell emission in previous laser experiments [3]. Argon is not a practical tracer, but potassium ($Z=19$) is. Its K_α features (Be-like, B-like) are centered near $3.6\ \text{\AA}$. Uranium ($Z=92$) M-shell emission is too hard to effectively backlight the potassium, but based on its atomic number, we determined that thorium ($Z=90$) would be a good candidate. It is also the only readily available material with atomic number between 83 and 92. We purchased bismuth and thorium foils from Goodfellow Metals to use as the backlighters.

The hohlraums were supplied by GA. They were thin-walled cylindrical hohlraums, $1500\ \mu\text{m}$ by $3500\ \mu\text{m}$. This relatively large length was intended to allow us to fit three OMEGA cones into the hohlraum, and keep all of the beams sufficiently far from the witness plates and the various diagnostic holes. We estimated the hohlraum temperatures from the simple scaling relationship in Ref. [7]. We were unfortunately unaware at this time of the result illustrated in Figure 3 of Ref. [8], which shows that hohlraum temperature decreases when beams are pulled back from the hohlraum midplane and toward the laser entrance holes (LEHs). We chose depths for the tracers based on this high estimate of the hohlraum temperature. We have since developed a view factor code which confirms the lower hohlraum temperatures in detail.

The hohlraums were prepared by Russell Wallace at Livermore. He drilled either a DANTE hole (for the shock breakout targets) or a backlighter hole (for the tracer spectroscopy targets) in the hohlraums, as well as two holes in each flat. He also assembled the shock breakout targets by gluing pairs of doped and undoped wedge witness plates onto the flats. Pete Gobby at Los Alamos assembled the tracer targets, which also involved attaching pairs of witness plates to the flats. The main challenge posed by these targets

was the backlighters, however. They were attached to the barrels of the hohlraums by a wire, such that the two 1 mm square foils were about 3 mm from the hohlraum midplane. The vast majority of the targets were aligned well within the tolerances which enable proper placement of the two backlighter spots. Finally, plastic shields were glued on the ends of the hohlraums to prevent the main diagnostics from seeing LEH plumes.

We also built several foil-only targets, for measurements of the unattenuated backlighter spectra, and KCl disk targets for performing wavelength calibrations. In Figure 3 we show snapshots of the two different types of hohlraum targets, taken with the LLE Powell scope.

We would like to note at this point that we had an extraordinary amount of support from the ICF community in order to develop and build these targets. The support went beyond advice and encouragement, when the cost of the targets relative to our budget increased drastically. With the generous help of the target managers from the national labs, the Wisconsin Foundation, and accommodation by GA, we were able to build 24 hohlraum targets.

3. Diagnostics

The side-by-side tracer spectroscopy technique required a spectrometer that could provide moderate resolution ($\lambda/\Delta\lambda \approx$ a few $\times 100$) of the two wavelength regions near the K_α features from potassium and chlorine, respectively. A curved crystal seemed like a natural choice to cover the range from 3.4 Å to 4.8 Å, but we were concerned about achieving the throughput necessary to make a meaningful time-resolved measurement. We therefore designed a spectrometer with two flat crystals, each to focus on a narrow spectral range that covered most of the K_α features from each of the two tracers. Although the narrow spectral range could make it difficult to establish an accurate wavelength scale, and might cause some data to be lost if the crystals were not aligned well enough, this scheme has an order of magnitude higher throughput than a scheme using a curved crystal.

We used a PET crystal with the potassium tracer and thorium backlighter and an ADP crystal with the chlorine tracer and bismuth backlighter side. We estimate an instrumental resolution of $\lambda/\Delta\lambda \approx 200$ for the PET and $\lambda/\Delta\lambda \approx 500$ for the ADP. The signal from the two crystals illuminated a CsI photocathode and the data were recorded on a streak camera. This diagnostic, dubbed the LXS, was built by David Hoffman at the University of Wisconsin Space Astronomy Laboratory shop. It was fielded in TIM 1.

For the shock breakout measurement, we used the new streaked optical pyrometer (SOP), which was built and fielded by John Oertel of Los Alamos. Our campaign in August 1998 was, in fact, the first time the SOP was used for target shots. It imaged the back of our wedge witness plates, detecting self-emission near 3000 Å when the shock broke out. The data were recorded on a CCD, with a nominal time resolution of 10 ps and a spatial resolution of 5 μm . In practice, the resolution was expected to be limited by the signal-to-noise. The SOP was fielded in TIM 5.

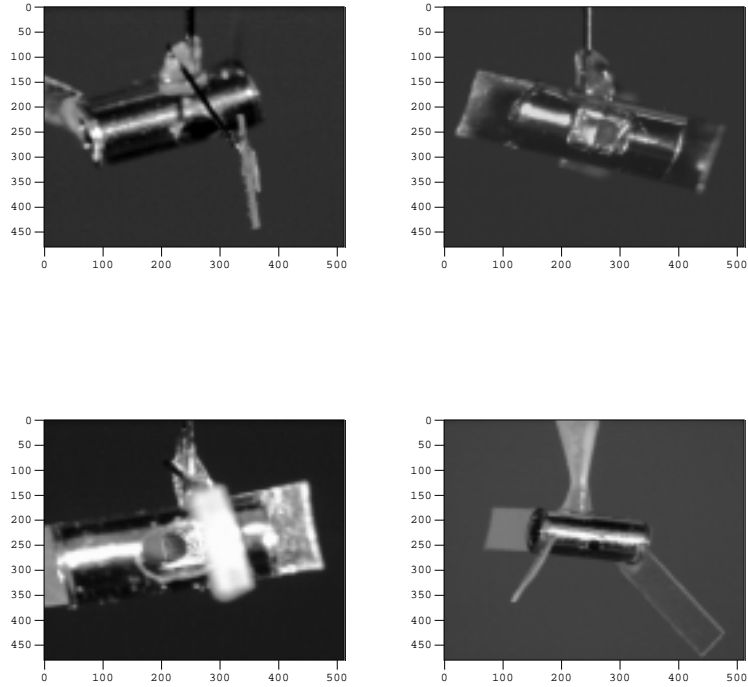


Figure 3. In the top row we show images of a tracer spectroscopy hohlraum target, as seen from the backlighter side (left) and witness plate side (right). Note that the foil hangs off of the hohlraum barrel from a wire, and that a large hole has been drilled in the barrel to allow the backlighter photons to propagate through the hohlraum. The difference between the doped and undoped witness plates can be seen in the somewhat milky appearance of the germanium doped sample. In the bottom row on the left we show the same tracer spectroscopy target from an angle that allows one to look through the backlighter hole and view the witness plates from the inside. On the lower right we show a shock breakout target, with its DANTE hole visible (the wedge witness plates are on the back side). In all these images the plastic LEH shields are prominent.

Table 2. Beam Pointings

Cone	Angle (degrees)	Beam Lines	Pointing ^a (μm)	Focus ^b (μm)	Spot Position ^c (μm)
2	47.8	H6 side: 11, 15, 23, 24, 31, 39 H15 side: 49, 52, 53, 54, 62, 65	1700	0	915
3a	58.8	H6 side: 12, 13, 28 H15 side: 43, 55, 57	1600	-500	1145
3b	62.3	H6 side: 14, 16, 17, 18, 21, 22 H15 side: 41, 45, 47, 48, 58, 64	1650	-500	1255

^aDistance from the LEH midplane along the long axis of the hohlraum.

^bDistance toward the target chamber center from the pointing position.

^cDistance from the hohlraum midplane.

The DANTE was also used on the shock-breakout shots. A fast framing camera was used to monitor the beam locations both in the hohlraum and on the backlighter, as well as hole closure of the DANTE diagnostic hole.

4. Experiments and Data

The day before the experimental campaign began, we metrologized the targets using the Powell scope at LLE. Primarily we did this to verify the alignment of the backlighter and witness plates and the positioning of the shields. We also used the Powell scope and camera to make images of what the targets looked like as seen from the various diagnostic ports and the TVY and TVX monitors to aid in aligning the targets in the target chamber.

We used the H6-H15 axis for all of the hohlraum targets, with the LXS in TIM 1 and the SOP in TIM 5. We put 30 beams from cones 2, 3a, and 3b into the hohlraums. The six cone 1 beams on the H15 side were used to illuminate the backlighter foils (and were unused in the shock breakout shots). The three cones were brought into focus near, but not exactly in, the LEH plane and resulted in three closely spaced but non-overlapping rings on each side of the hohlraums. The beam pointings are summarized in Table 2.

4.1. Shock Breakout Shots

As we mentioned above, the LANL SOP was being used for the first time. On the first several shots no signal was measured. Finally on the last shock breakout target we changed the filter, and measured a relatively strong signal. The signal, while generally sensible, appeared to be out of focus. We show the data from this shot in Figure 4. It was eventually determined that the optics were indeed out of focus, because the offset in position of the witness plate from the target chamber center was not taken into account when the SOP was being set up. Although this distance was less than 1 mm, the SOP’s optics are very fast and the depth of field was actually less than this offset. The out of focus data from this last shock breakout shot does, however, show the qualitative details we expect, indicating that a meaningful time-dependent measurement of the shock breakout from each of the two witness plates can be made with the SOP.

DANTE data was collected for each of the shock breakout shots. In several of the shots DANTE was saturated by emission from the LEH plumes such that the shields failed to block. This was because we left very little tolerance for error in the angle specifications of the shields. We were concerned about two of the beams hitting the shields and not depositing their energy in the hohlraums, so we opted to make the shield angles as large as possible. The actual shield angle variation was ± 2 degrees, which was what we were told to expect. In our next campaign, we will place the shields more conservatively, and turn off one or two beams on each side.

4.2. Spectroscopy Shots

The LXS and streak camera functioned well almost immediately at the start of the campaign. We took a relatively strong spectra of the bismuth and thorium backlighter foils (without any hohlraums). The M-shell pseudocontinua were relatively smooth, as can be seen in Figure 5. However, by shooting the Bi and Th separately, we also noticed that the Bi signal is picked up to a certain extent near 3.6 Å in the PET crystal, as well as in the ADP crystal near 4.6 Å. There was much less of a problem with the Th emission being seen in the ADP crystal.

The K and Cl emission features (He-like and Li-like satellite) in the calibration shots indicated that the spectral range for each crystal corresponded only to about five ionization stages.

In the “integrated” shots, with hohlraums, witness plates, and backlighters, we noticed that the germanium dopant added significantly to the opacity of the witness plates to the backlighter photons. This effect should be mitigated in future targets by making the witness plates thinner. The other problem we noticed with the integrated shots was an unwanted spectral signal due, we think, to the gold M-band emission from laser hot-spots. This problem should be eliminated by using thick-walled hohlraums.

Unfortunately, we did not measure a spectral signal in any of these integrated shots. We were concerned that our target design was flawed, but compared to the DANTE-derived temperatures, the predicted temperatures were high. These lower temperatures led to lower velocities, and therefore the radiation wave did not arrive at the depth of the tracers before

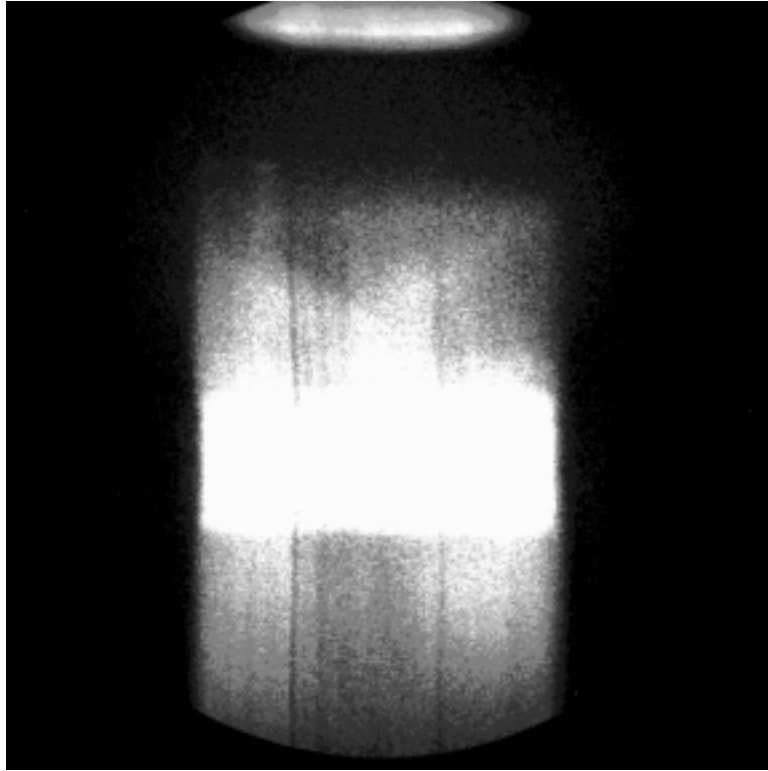


Figure 4. Time goes down along the y-axis in this CCD image taken with the LANL SOP for OMEGA shot number 13614. The x-axis is a line across the two witness plates, which have their thickest ends abutting in the middle of the image, and the thin ends on either side. A faint and ill-defined (due to the focus problems) “V” shape in the data is caused by the shock breaking out (and hence the rear of the witness plate radiating) first at the thin ends of the witness plates, which is seen on each side of the film, and then proceeding inward toward the middle of the film at later times. The brighter signal above the “V” *before* the shock breaks out on the right side is likely due to preheat as the right side corresponded to the location of the undoped witness plate in this shot. The burst of signal at early times is probably due to reflected laser light propagating through the cool and transparent witness plates at early times. The brightening at later times is due to the radiation wave reaching the back of the witness plates.

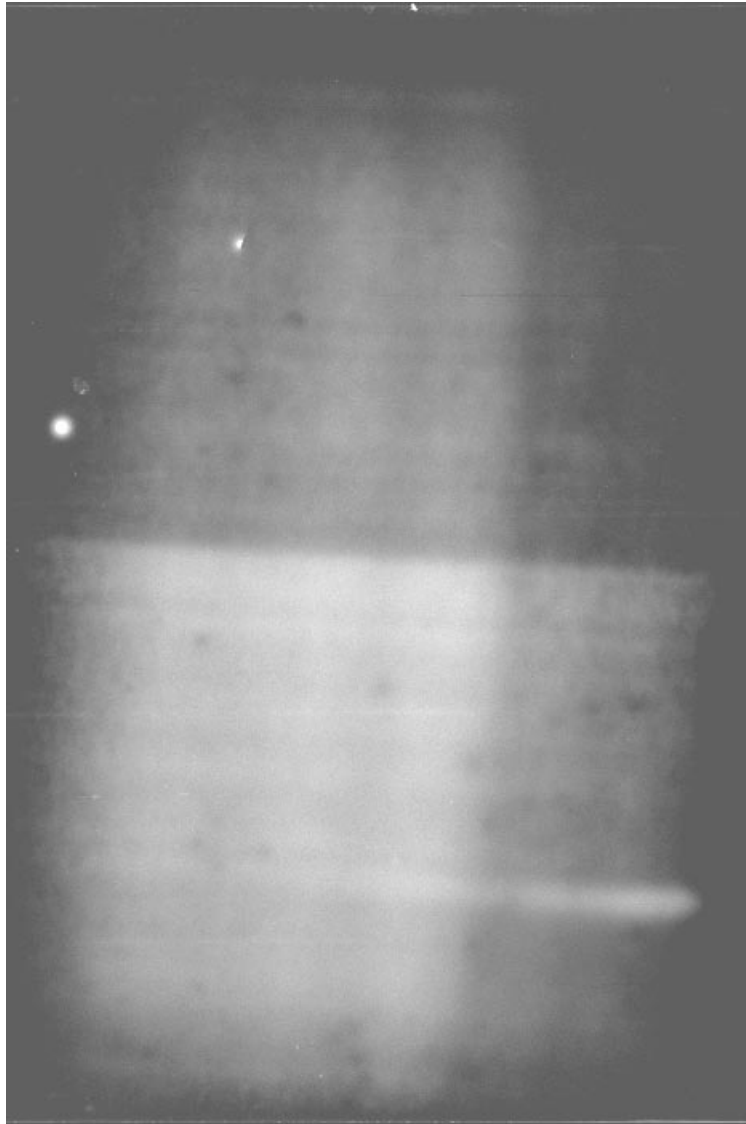


Figure 5. From shot number 13628, bismuth and thorium M-shell spectra, with the Bi in the top half, wavelength increasing down, and Th in the bottom half, also with the wavelength increasing down. Time increases to the left. Note that the beams irradiating the backlighter foils were staggered, and the brightening some time after the initial signal is due to the second and third beams being turned on. Note that these backlighter spectra are quite smooth.

the drive itself shut down. The lower-than-predicted drive temperatures, as we discussed in the previous section, were due to the beam pointings, which were pulled back from the midplane in our relatively long hohlraums.

5. Discussion and Conclusions

We presented the results of the August 1998 experiments at the APS DPP meeting in New Orleans in November 1998. The first poster we presented at this meeting consisted of a description of the experiments and a display of some of the data and simulations. The second poster focused on characterizing the hohlraum radiation field using the 3-D view factor code, SYMRAD, we recently developed [9].

The view factor calculations (an example of which is shown in Figure 6) confirmed the relatively low drive temperatures measured by DANTE (peak wall temperatures of approximately 155 eV before applying an albedo correction). Radiation-hydrodynamics simulations and CRE/spectral post-processing confirmed that at these drive temperatures and given the tracer depths we used ($> 15 \mu\text{m}$), the radiation wave did not reach the tracers until the drive was off. This resulted from the fact that the peak temperatures in our stretched hohlraums were 25 eV lower than we had anticipated. Thus the temperatures of the tracers were never high enough to generate ionization stages with vacant L-shells which are capable of giving rise to K_α transitions. These same simulations showed that if the tracers were placed at a shallower depth (approximately $8 \mu\text{m}$) or if the hohlraum temperatures were higher (by 10 to 15 eV), we would have seen the K_α absorption signals while the drive was still on.

The specific conclusions from the view factor modeling of our hohlraums included: (a) by modeling the time- and temperature-dependent hohlraum albedo with our radiation-hydrodynamics code, we are able to get good agreement between the view factor simulations and the DANTE data; (b) the temperature gradient across the witness plates were roughly 1.5 eV per 100 μm ; (c) losses from the backlighter hole served to lower the hohlraum temperature by 3 to 4 eV; and (d) the effect of pulling the beams back from the hohlraum midplane and toward the LEHs was significant (3 eV per 100 μm), but somewhat weaker than that reported in standard scale-1 hohlraums [8].

As part of our CRE/spectral modeling effort, we discovered that K_β features are quite sensitive to tracer temperature at very low temperatures (2 eV can be easily discriminated from 3 eV). This is especially true for chlorine, where even the neutral atom has an M-shell vacancy. Its usefulness as a diagnostic depends on continuum lowering destroying bound states above $n = 4$, so that only a few lines are seen from each ionization state. This condition should hold at solid density.

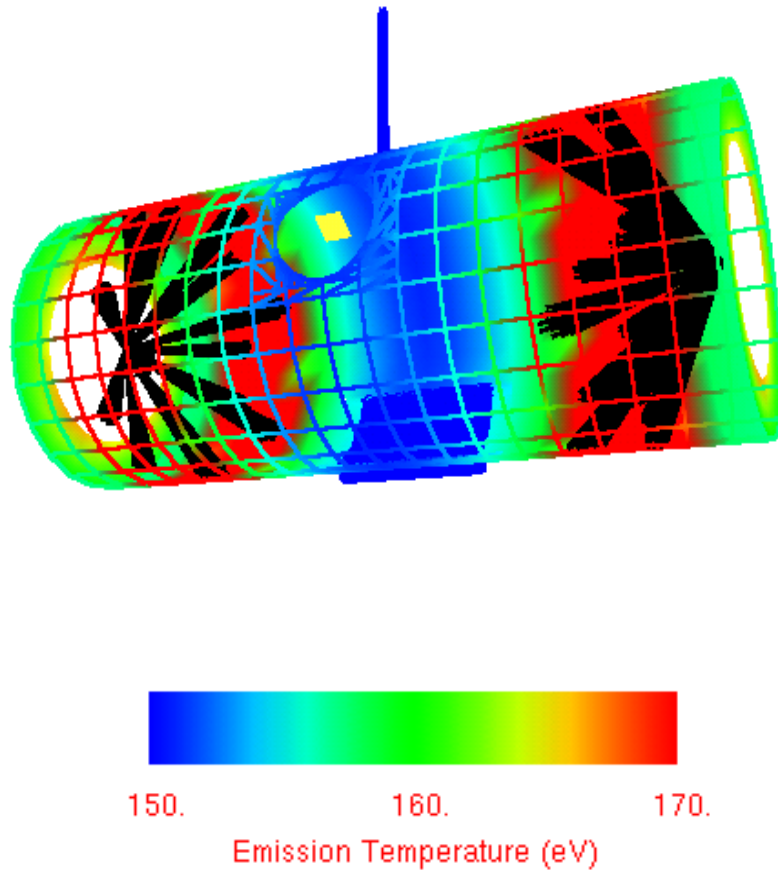


Figure 6. SYMRAD 3-D view factor simulation of one of our hohlraums, irradiated by 30 OMEGA beams. In these simulations, we are able to compute the time-dependent temperature distribution inside the hohlraum.

We close by summarizing the important results from the FY1998 effort:

- Layered planar plastic targets with thin tracer layers can be reliably fabricated using the GDP process.
- The finished witness plates can be effectively characterized, in terms of the thicknesses of the layers, their density, and their surface roughness.
- Backlighter foils can be reliably attached to the hohlraum barrels, and using a hole opposite the witness plates, can be aligned with the witness plates and spectrometer.
- Bismuth and thorium foils, illuminated by three OMEGA beams, produce good pseudocontinuum backlighter sources.
- Shields for the diagnostics are crucial for blocking emission from LEH plumes.
- Spectra from two packages can be simultaneously observed using a double point backlighter and the LXS.
- The SOP can be used to make a single time-resolved measurement of the shock breakout from two side-by-side wedges.
- DANTE measurements in conjunction with detailed numerical modeling are important for characterizing the hohlraum radiation field.
- Tuning the tracer placement to the actual drive profile, which can be affected by the beam pointing, is crucial for measuring K_{α} absorption signals.

These conclusions will be brought to bear on the next round of experiments, to be performed in July 1999. Specifically, we have redesigned the hohlraums and adjusted the tracer depths in order to optimize the signal from the tracers, and thus, make a meaningful radiation-wave timing comparison between doped and undoped ablator samples.

Acknowledgements

We would like to thank John Soures and the NLUF program for supporting this work. We are grateful for the help we received from Dave Hoffman, Mark Bonino, Garth Pratt, Bob Turner, Pete Gobby, Russ Wallace, Paul Cahill, Ken Schultz, Abbas Nikroo, Jim Kaae, Harry Bush, Dave Hebron, Ray Leeper, Elsayed Mogahed, Gerald Kulcinski, and Greg Pien, Sam Morse, and the rest of OMEGA Operations.

References

1. Hauer, A. A., Delamater, N. D., and Koenig, Z. M., *Laser and Particle Beams*, **9**, 3 (1991).
2. Perry, T. S., et al., *J. Quant. Spectrosc. Radiat. Transfer* **51**, 273 (1994).
3. Chenais-Popovics, C., et al., *Phys. Rev. A* **40**, 3194 (1989).
4. MacFarlane, J. J., Wang, P., Bailey, J. E., Mehlhorn, T. A., and Dukart, R. J., *Laser Part. Beams.*, **13**, 231 (1995).
5. Dittrich, T. R., et al., *Phys. Plasmas*, **6**, 2164 (1999).
6. MacFarlane, J. J., Cohen, D. H., Wang, P., Peterson, R. R., Moses, G. A., Back, C. A., Landen, O. L., Leeper, R., Olson, R. E., and Nash, T., *UWFDM-1069* (<http://fti.neep.wisc.edu/FTI/pdf/fdm1069.pdf>) (1998).
7. Lindl, J. D., *Phys. Plasmas* **2**, 3933 (1995).
8. Decker, C., et al., *Phys. Rev. Lett.* **79**, 1491 (1997).
9. MacFarlane, J. J., *UWFDM-1061* (<http://fti.neep.wisc.edu/FTI/pdf/fdm1061.pdf>) (1998).